Annu. Rev. Fluid Mech. 2000. 32:445–476

SONOLUMINESCENCE: How Bubbles Turn Sound into Light

S. J. Putterman and K. R. Weninger
Physics Department, University of California, Los Angeles, California 90095; e-mail: putterman@physics.ucla.edu

Key Words energy focusing, nonlinear dynamics, complexity, hydrodynamics gas bubble, continuum mechanics, shock shape instabilities, chemical hydrodynamics

■ **Abstract** Sonoluminescence, the transduction of sound into light, is a phenomenon that pushes fluid mechanics beyond its limit. An initial state with long wavelength and low Mach number, such as is realized for a gas bubble driven by an audible sound field, spontaneously focuses the energy density so as to generate supersonic motion and a different phase of matter, from which are then emitted picosecond flashes of broad-band UV light. Although the most rational picture of sonoluminescence involves the creation of a ''cold'' dense plasma by an imploding shock wave, neither the imploding shock nor the plasma has been directly observed. Attempts to attack sonoluminescence from the perspective of continuum mechanics have led to interesting issues related to bubble shape oscillations, shock shape instabilities, and shock propagation through nonideal media, and chemical hydrodynamics. The limits of energy focusing that can be achieved from collapsing bubbles in the far-off equilibrium motion of fluids have yet to be determined either experimentally or theoretically.

INTRODUCTION: LIGHT FROM FAR-OFF EQUILIBRIUM FLUID MOTION

Sonoluminescence (SL) is a unique phenomenon in fluid mechanics because it evolves out of an initial state within the range of parameters described by the basic equations of Navier Stokes hydrodynamics (Landau & Lifshitz 1987) into a different phase of matter—one with a remarkably high energy density whose characterization requires a completely different set of equations. In particular an imposed sound wave with a Mach number that is small compared with unity and a wavelength that is large compared with the mean free path can, in the presence of a bubble, focus its energy in a runaway fashion so as to generate picosecond flashes of broad-band UV light (Barber & Putterman 1991, Hiller et al 1992, Hiller et al 1994, Barber et al 1997a, Putterman 1998, Crum 1994, Putterman 1995). The energy of a UV photon compared with that of a single atom vibrating

in the imposed sound field represents an energy focusing that spans 12 orders of magnitude.

Nature's tendency to focus energy in the off-equilibrium motion of fluids is spectacularly robust. Figure 1 shows a photo of a single bubble attached to a wire in an acoustically excited fluid (Weninger et al 1997). Owing to the boundary conditions imposed by the wire, the bubble is not spherical but is distorted into an approximation of a hemisphere. Yet this bubble pulsates synchronously with the sound field, expanding during the rarefaction part of the acoustic cycle and collapsing so strongly during the ensuing compression that the input acoustic energy is transduced into UV flashes of light—one flash for each cycle. Figure 2 (see color insert) is an actual photo of the luminescence from a spherical probe

Figure 1 A hemispherical bubble trapped on a 500-μm wire in a sound field emits UV flashes of light and damages the metallic surface of the wire. It is not known whether this effect is caused by an imploding (hemispherical) shock, a jet, (Prosperetti 1997) or some other unidentified process.

vibrating at about 25 kHz in water. Bubbles spontaneously appear near the probe at the maxima of the dipolar sound field that the probe generates. Despite distortions caused by other bubbles and by the probe itself, these bubbles collapse with sufficient force to generate UV light. The local heating, which is 15 orders of magnitude greater than follows from Kirchoff's law for the attenuation of sound, is strong enough to lyse cells. In fact this device is regularly used for the surgical procedure called ultrasonically assisted liposuction (Weninger et al 1999a). In that case a small hole up the center of the probe is used to remove the emulsified fatty tissue. This version of SL closely resembles the configuration used in its discovery in 1934 (Frenzel & Schultes 1934, Walton & Reynolds 1984) and in sonochemistry (Suslick & Flint 1987, Long et al 1998).

When the pressure drop in flow through a Venturi tube exceeds 1 atm, bubbles spontaneously form and then later emit a flash of light as they collapse downstream (Putterman 1998, Peterson & Anderson 1967, Weninger et al 1999b). In all of these cases the bubbles emit light with the same spectral density as SL. The spectrum is broad band out to photon energies of 6 eV (wavelengths of 200 nm), where it is cut off by the extinction coefficient of water. The case that is most amenable to experimental measurement is that of a single gas bubble trapped at the velocity node of an acoustic resonator (Barber & Putterman 1991, Temple 1970, Gaitan et al 1992) (Figure 3, see color insert). In this case the system can be tuned so that the flashes come out with a clocklike synchronicity—one flash for each cycle of sound with the jitter in the time between flashes <50 ps (Barber et al 1992).

Early explanations of the light-emitting mechanism for SL-invoked frictional electricity (Frenzel & Schultes 1934). This phenomenon is illustrated in Figure 4 (see color insert), where one sees light emitted along the line where the meniscus of mercury meets the wall of a rotating glass cell (Picard 1676). These spectra are not broad band but have lines characteristic of electric discharges. Probably static electrification is not the explanation for SL. But this photo is another example of energy focusing in the off-equilibrium motion of a (non-Newtonian) fluid. For rotational rates of 1 revolution per minute, electrons are continuously separated and accelerated to 1% of the speed of light and discharged in picosecond bursts with energies of $\geq$20eV (Budakian et al 1998). The mechanisms underlying triboelectrification are still under investigation (Terris et al 1989).

PHENOMENOLOGY OF SONOLUMINESCENCE

Key to SL is the radius R as a function of time t for a single bubble pulsating in an imposed sound field. Figure 5 shows a typical $R(t)$. The bubble starts off from an ambient radius of $R_0 = 5.75$ μm, which is the radius at which the bubble is in static mechanical equilibrium with the external ambient pressure (typically 1 atm). As the applied sound field goes negative beyond an atmosphere in the region indicated by t_A, the bubble expands. When the total pressure acting on the bubble

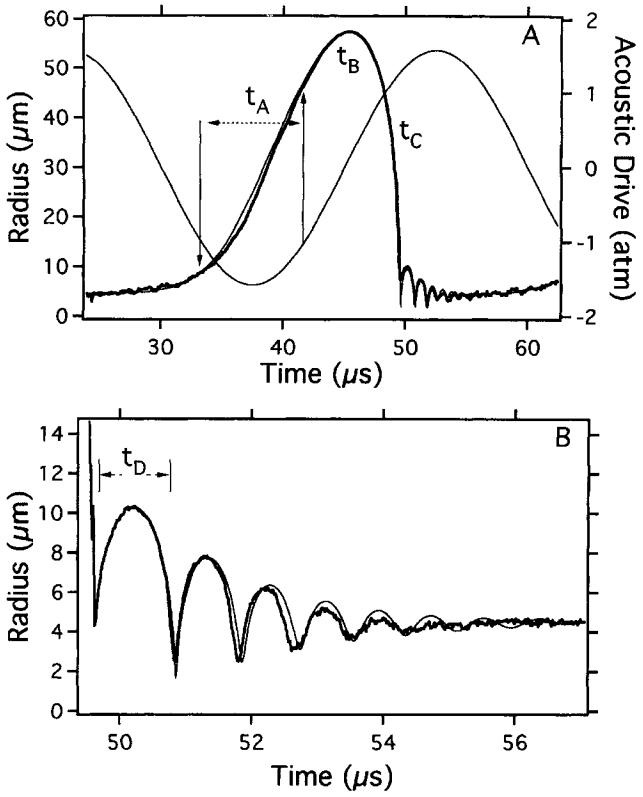

Figure 5 Radius versus time for a typical sonoluminescing bubble. Shown is a 3-torr argon bubble with $R_0 = 5.75$ μm and $P_a = 1.58$ atm. The ambient temperature is 10°C and, for the purpose of modeling the damping, the viscosity has been set to 0.05 cm^2/s. (A) A full cycle of sound. (B) The afterbounces.

becomes positive again, the bubble continues to expand for a time t_B, owing to its inertia, and then finds itself perched at a maximum radius $R_m \approx 10\ R_0$, when the total pressure has once again become equal to 1 atm. At this point the volume of this bubble has increased a factor of 1000 from its ambient value, and so its internal pressure has gone down about a factor of 1000. The near vacuum in the bubble cannot withstand the 1 atm from outside, and so the bubble catastrophically collapses in a manner first calculated by Rayleigh in 1917. The collapse is arrested as the bubble approaches its van der Waals hard core (roughly $R_0/9$), as shown in Figure 6, which is an enlargement by a factor of 1000 of the time scale in Figure 5*A*. At this moment of extreme stress and heating, the bubble's contents have approached solid densities, and the flash of light is emitted. Also shown in Figure 6 is the fact that the collapse velocity of the bubble reaches over four times the ambient speed of sound in the gas. And, as shown in Figure 7, which is a

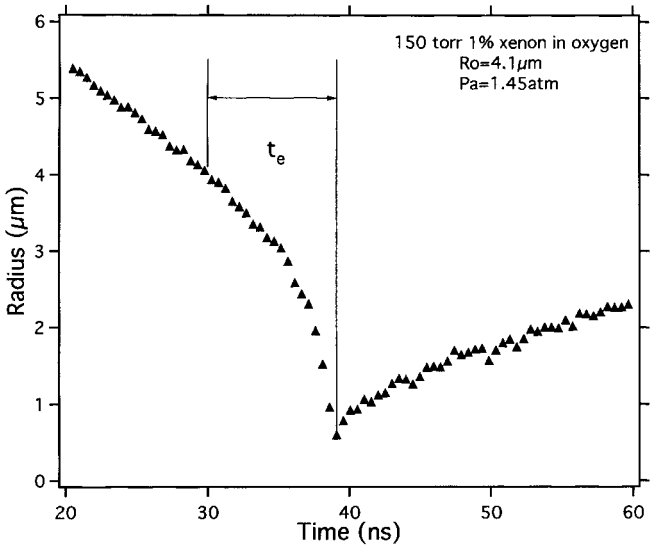

Figure 6 Radius versus time as the bubble collapses supersonically toward its van der Waals hard core. The data are taken for a 150-torr 1% xenon-in-oxygen bubble with $R_0 = 4.1$ μm and $P_a = 1.45$ atm. The temporal resolution of 500 ps is achieved with pulsed Mie scattering (Barber et al 1997a). To apply Mie theory, the index of refraction of the gas in the bubble has been reckoned to unity.

sixfold enlargement of the Figure 6 time scale, the acceleration at the turnaround exceeds 3×10^{11} *g*. After the light emission, the bubble pulsates freely (Figure 5*B*) and then sits dead in the water waiting for the next cycle, when this all repeats with remarkable synchronicity.

The spectrum of SL from a helium bubble in water is shown in Figure 8. These data display the strongly UV spectrum as well as the sensitivity to temperature. Colder water makes for a much stronger light emission (Hiller et al 1992). Typically as the water is cooled from 30°C to 0°C, the intensity of SL increases by a factor of ~100 with emissions at 0°C ranging up to 10^7 photons per flash.

So far it has been determined that SL in water is sensitive to the particular gas used, the ambient temperature and pressure, the partial pressure at which the gas has been dissolved into the water, and the acoustic amplitude. So far the effects of changing the acoustic frequency (typically 12–45 kHz) appear to be comparatively small. The flash widths for various parameters are shown in Figure 9. They range from 30 ps for well-degassed air in water to >200 ps for xenon bubbles in cold water (Gompf et al 1997, Hiller et al 1998). An important aspect of the flash is that its width is independent of color (as measured so far for air and helium bubbles). The flash width at 200 nm is within a few percent of the flash width at 800 nm. This measurement challenges any adiabatic theory of light

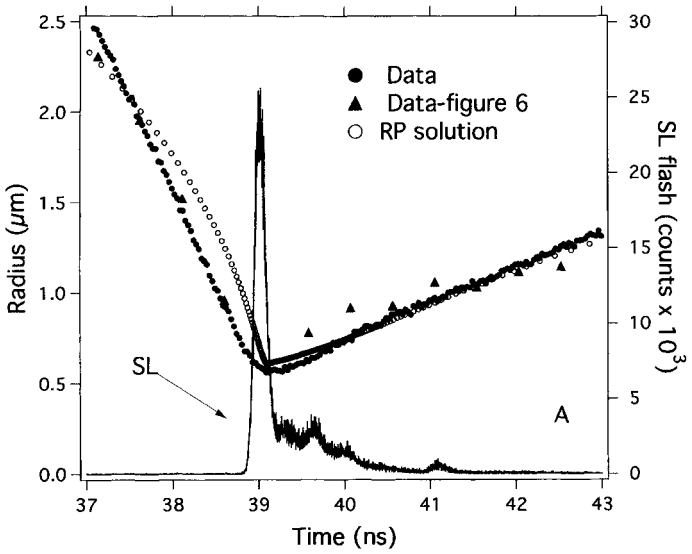

Figure 7 Radius versus time near the minimum radius with an overlay of the sonoluminescence flash for 150-torr 1% xenon in oxygen at 40 kHz. The 25-ps resolution in *A* is achieved with time-correlated single-photon counting (O'Connor & Phillips 1984) applied to pulsed Mie scattering. For comparison $R(t)$ from Figure 6 is overlaid. Application of time-correlated single-photon counting to the SL flash (Gompf et al 1997) determines a width of 150 ps (Hiller et al 1998) for this system. Also shown is a solution of Rayleigh's equation of bubble motion. In *B* the uniform adiabatic heating implied by the Rayleigh-Plesset equation (taking $C_p/C_v = 5/3$ and using the van der Waals equation of state) is compared with the SL flash. The afterpulsing is an artifact of the tube. For the RP simulation, $R_0 = 4.1$ μm and $P_a = 1.45$ atm. Light for the Mie scattering measurements was collected from a large solid angle, and small diffractive corrections were not made to these data.

emission, because smooth heating and cooling would lead to longer emissions of low-energy photons.

If the argon that constitutes 1% of air is removed, the light emission becomes very weak and unstable (Hiller et al 1994). In general SL from oxygen and nitrogen is very difficult to achieve, unless they are mixed with some noble gas. Hydrogenic gases also pose challenges, but in well-controlled resonators these bubbles can glow for about a minute or longer (Barber et al 1995, Löfstedt et al 1995). Hydrogenic bubbles are significantly more stable than oxygen and nitrogen. Also, whereas 1% argon added to oxygen or nitrogen dramatically improves the light emission and stability, such a small dosing has no observable effect on a hydrogen bubble (Barber et al 1997a).

Finally xenon plays a special role. In SL from a single bubble, xenon yields the brightest emission, ~fivefold brighter than helium bubbles. In alcohols (Wen-

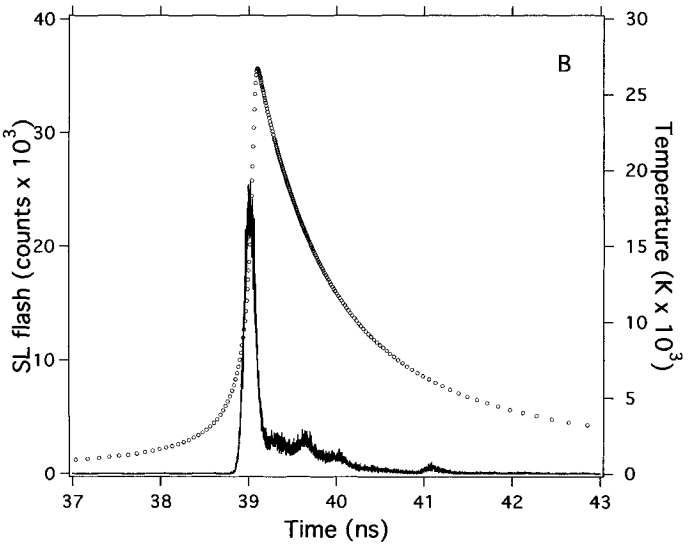

Figure 7 Continued

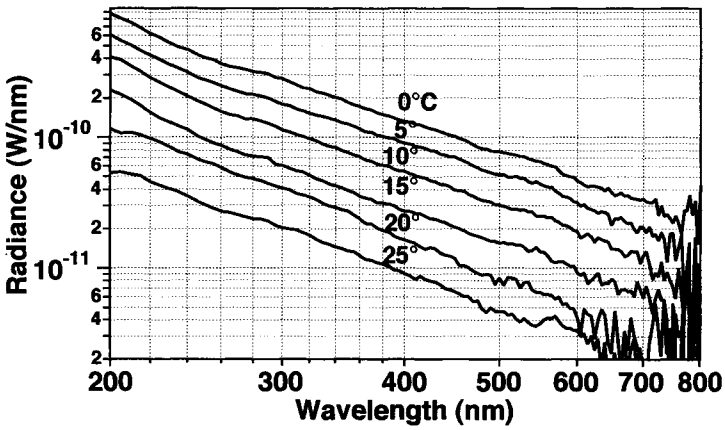

Figure 8 Spectrum of SL from a helium bubble. Data for energies of >6 eV (wavelengths < 200 nm) have not been obtained owing to poor transmission through water.

inger et al 1995), Venturi flow, and the collapse of distorted bubbles such as shown in Figures 1 and 2, xenon can lead to an increased output of light by a factor >1000.

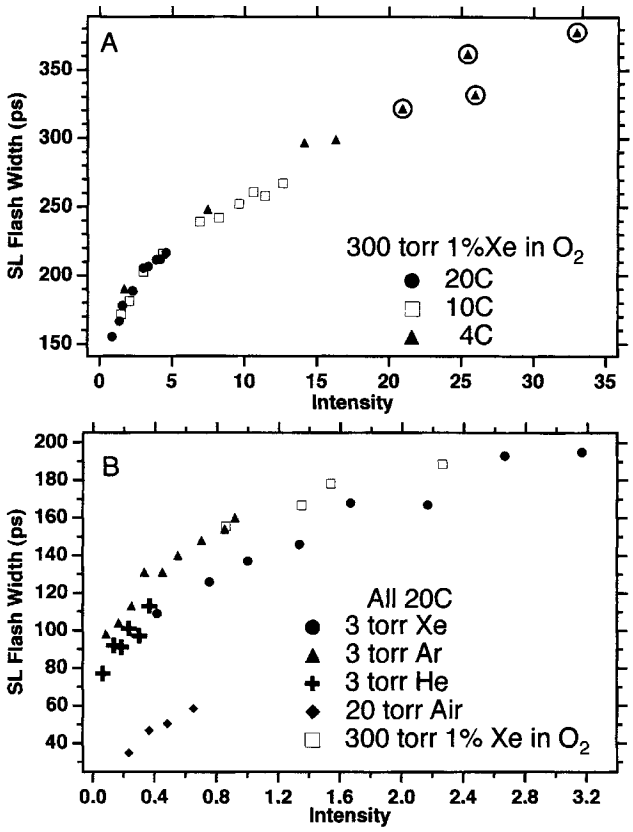

Figure 9 Flash width of sonoluminescence as a function of intensity of emission for various temperatures (top) and gas mixtures (bottom) at 500 nm.

TIME SCALES FOR BUBBLE MOTION

Figures 5 and 6 indicate a number of time scales that characterize the mechanical pulsating motion of the bubble. These time scales can be interpreted from Rayleigh's equation of bubble motion (commonly called the Rayleigh-Plesset or RP equation), which we now discuss.

In the limit at which the imposed sound field $P_a(r, t)$ has a small Mach number, such that $|P_a/\rho c^2| \ll 1$, where c is the speed of sound in the fluid (c_0 will denote the speed of sound in the gas), and the Mach numbers of the bubble are small, $\dot{R}/c \ll 1$, and the wavelength of the sound field, $\lambda = 2\pi/k$, is large compared with the bubble radius, $kR \ll 1$, one is led to the leading-order RP equation (Rayleigh 1917; Prosperetti 1984; Prosperetti & Lezzi 1986, 1987; Löfstedt et al 1993):

$$R\ddot{R} + \frac{3}{2}\dot{R}^2 = \frac{1}{\rho}[P_g(R) - P_0 - P_a(0, t)] - \frac{4\eta\dot{R}}{\rho R} - \frac{2\sigma}{\rho R} + \frac{R}{\rho c}\frac{d}{dt}(P_g - P_a). \quad (1)$$

The left-hand side of this equation represents the inertia of the accelerating bubble in response to the net force on it, which, as on the right-hand side, is caused by the difference in pressures inside and outside the bubble. At leading order, the damping is caused by viscous effects and the radiation of sound into the fluid by the bubble's motion. The externally imposed (sinusoidal standing-wave) sound field at the bubble is

$$P_a(0, t) = P_a' \cos \omega_a t, \quad (2)$$

where P_a' includes the response of the resonator to the drive.

The RP equation needs to be supplemented with an equation of state for the gas, so that it becomes a closed equation for $R(t)$. For rapid changes in the bubble radius, we use the adiabatic equation of state (Barber et al 1997a, Löfstedt et al 1993):

$$P_g(R) = \frac{P_0 R_0^{3\gamma}}{(R^3 - a^3)^\gamma}; \; T_g(R) = \frac{P_0 R_0^{3(\gamma-1)}}{(R^3 - a^3)^{\gamma-1}}, \quad (3)$$

where $\gamma = C_p/C_V$, the ratio of specific heats, and we have allowed for the possibility that the collapse is sufficiently strong that the hard-core radius of the bubble contents, a, is probed. This radius is related to the van der Waals excluded volume, b, by $4\pi/3\, a^3 = \mathfrak{n}b$, where $\mathfrak{n}$ is the number of moles in the bubble and for air $b = 0.04$ l/mole, so that, for air, argon $R_0/a = 8.5, 8.8$. For slow motion (such as when the bubble is expanding during the time scale t_A), we assume an isothermal equation of state, $P_g(R) = P_0 R_0^3/R^3$; $T_g(R) = T_0$, where T_0 is the ambient temperature. In general the subscript g denotes properties of the gas, and the subscript 0 denotes properties of the gas at ambient conditions. Use of the adiabatic equation of state assumes that the state of the gas inside the bubble is uniform, which requires that the speed of the bubble wall be small compared with the speed of sound in the gas, $\dot{R}/c_g \ll 1$.

The RP equation enables us to calculate the various time scales governing the SL bubble's dynamics (Barber et al 1997a). To characterize the expansion of the bubble from its ambient radius to the maximum radius, the RP equation is expanded around the maximum rarefaction of the drive to obtain (Apfel 1986)

$$\dot{R}_A = \left[\frac{2}{3}\frac{(P_a' - P_0)}{\rho}\right]^{1/2}, \quad (4)$$

corresponding to a Mach number relative to the ambient speed of sound in gas $M = 0.01$ for typical $P_a' \approx 1.4$ atm. The time scale t_A is therefore

$$t_A \approx (R_m - R_0)/\dot{R}_A, \tag{5}$$

in agreement with Figure 5. Owing to the inertia of its expansion, the bubble continues to grow even after the net pressure acting on it is no longer negative. This is the time scale t_B associated with its turnaround at the maximum radius. Expanding the RP equation around this radius yields

$$t_B \approx \left(\frac{\rho R_m^2}{P_0}\right)^{1/2}, \tag{6}$$

which is ~5 μs (in agreement with Figure 5). If this time scale is comparable to the time t_- required for the sound field to go from $-P_0$ to 0, then the bubble will find itself perched at its maximum radius with a vacuum on the inside and P_0 on the outside. So, if

$$t_B \sim t_- = (1/\omega_a)\sin^{-1}(P_0/P_a'), \tag{7}$$

the bubble at $R = R_m$ will be unstable against the collapse, which was first calculated by Rayleigh (1917). The time required for the bubble to collapse from its maximum radius to its minimum radius can be evaluated by neglecting damping and surface tension. Integrating this equation from R_m, where $\dot{R} = 0$, to R, and noting that, unless R is within 10% of the hard core a, the back pressure of the gas is negligible, yields

$$\frac{1}{2} R^3\dot{R}^2 + \frac{P_0(R^3 - R_m^3)}{3\rho} = 0. \tag{8}$$

For values of $R < R_m/2$, we have to good accuracy:

$$\dot{R} = -(2P_0/3\rho)^{1/2}R_m^{3/2}/R^{3/2}$$

$$\ddot{R} = -\frac{P_0 R_m^3}{\rho R^4}$$

$$R(t) = R(0)\left(1 - \frac{t}{t_0}\right)^{2/5}, \tag{9}$$

where

$$t_0 = \frac{2}{5}\left(\frac{3\rho}{2P_0}\right)^{1/2}\frac{R(0)^{5/2}}{R_m^{3/2}},$$

where t_0 is the time to go from the initial state $R(0)$ to the hard core radius. So that the time to go from $R_m/2$ to R_0 is

$$t_C \approx \frac{R_m}{10\sqrt{P_0/\rho}}, \tag{10}$$

and the time to go from R_0 to the minimum radius is

$$t_E \approx \frac{\sqrt{6}\ R_0^{5/2}}{5R_m^{3/2}\ (P_0/\rho)^{1/2}}. \tag{11}$$

For typical parameters, $t_C \approx 500$ ns and $t_E \approx 8$ ns, also in agreement with Figures 5 and 6 (Barber & Putterman 1992). Equation 9 involves only the approximation that the Mach number relative to the speed of sound in the fluid is small, $\dot{R}/c \ll 1$, so that the radius of the bubble must be larger than ~ 3 a. For such radii the effects of viscous damping and the back pressure of P_g can be neglected.

A linearization of Equation 1 around the ambient radius R_0 yields the dispersion law for the (adiabatic) radial pulsations of a free bubble with a frequency (Prosperetti 1984) of

$$\omega_0(P) = [3\gamma P/\rho R_0(P)^2]^{1/2}, \tag{17}$$

so that $t_D \approx 2\pi/\omega_0\ (P)$. Approximating P with P_0 and $R_0(P)$ with R_0 yields $t_D \sim 1.3$ μs for $R = 4.5$ μm. The difference between this estimate and the actual period (~ 0.75 μs) can be accounted for by the factor

$$\omega_0(P)/\omega_0 = [R_0/R_0(P)]^{5/2} = [P/P_0]^{5/6},$$

where P is the total pressure acting on the ringing bubble.

Finally, one can also use the RP equation to estimate the time for the bubble to turn around at its minimum radius by expanding Equation 1 around R_c. Using the parameters appropriate to SL, one finds a time scale of ~ 100 ps (Löfstedt et al 1993). However, this short time scale clearly lies outside the validity of the hydrodynamic approximations that led to the derivation of the RP equation. Such calculations serve only to show that these approximations are violated and that, although the RP is rich in mathematical implications at these parameters, it misses the physics essential to SL.

Another relevant time scale is the time it takes for heat to diffuse into the bubble, such as when the temperature changes owing to an adiabatic ringing. This time scale is ~ 1 μs (Prosperetti 1984, Löfstedt et al 1993), which is on the order of the time scale of the afterbounces. Thus the afterbounces are neither isothermal nor adiabatic, but the expansion of the bubble from R_0 to R_m (and the collapse back down to R_0) is sufficiently slow to be isothermal.

ENERGETICS OF SONOLUMINESCENCE

Acoustic energy entering the fluid causes the bubble to expand to a maximum radius R_m against the ambient pressure P_0. The energy stored in the bubble is

$$E_B = \frac{4}{3}\pi R_m^3 P_0. \tag{18}$$

As a specific example we consider a 300-torr, 1% Ar-in-N_2 bubble in water at

10°C so that $R_0 = 6$ μm and $R_m = 48$ μm and $E_B = 0.5$ erg (this bubble emits 2×10^6 photons per flash at a repetition rate of 30 kHz and is driven by a sound field with an amplitude of 1.4 atm). The bubble contains 2.25×10^{10} atoms or molecules of gas so that the potential energy stored per molecule is 14 eV (1 erg = 6.2×10^{11} eV and 1 eV = 11,600 K). It is this enormous energy per molecule that is cashed in when the bubble collapses to make SL. This large energy per molecule arises from a macroscopic potential being partitioned over a dilute gas (it has been assumed that any vapor in the bubble condenses out onto the wall during the collapse).

A typical resonator operating in its fundamental mode will be $\lambda/2$ on a side. The energy of the sound field E_a in this volume is about 100 E_B for a 30-kHz sound field ($\lambda \sim 5$ cm). Based on Kirchoff's law for the attenuation of sound, the amount of mechanical work dissipated into heat during each cycle is

$$\Delta E_K \approx \frac{\omega_a^2 \eta}{c^2 \rho} E_a T_a, \tag{19}$$

where T_a is the acoustic period, and the damping caused by viscosity has been retained. For the example under consideration, $\Delta E_K \sim 10^{-4} E_B$.

During the Rayleigh collapse, the acceleration of the bubble's volume radiates sound energy at frequencies ranging up to the gigahertz domain. In leading order ($\dot{R}/c \ll 1$, where c is the speed of sound in water), the scattered pressure field is

$$P_{sc} = \frac{\rho \partial (R^2 \dot{R})}{r \partial t}, \tag{20}$$

and the far-field acoustic energy radiated per second is

$$\dot{E}_{ac} = \frac{4\pi\rho}{c} \left(\frac{\partial}{\partial t} (R^2 \dot{R}) \right)^2. \tag{21}$$

According to Equation 9, the spectrum of sound radiated during the Rayleigh collapse drops off approximately as $(1/f)^{2/5}$, where f is the frequency of the radiated sound ($f \sim c/2\pi R$). This slow drop-off indicates that the integrated sound radiation is sensitive to the cut-off frequency at which the leading-order approximation breaks down. Because this will occur for $\dot{R} \sim c$, R will be measured in micrometers, and the radiated sound will indeed range up to ~1 GHz. So, in addition to the light, the bubble transduces the pure driving tone into a broadband burst of sound. Integrating Equation 21 by use of the solution to Rayleigh's equation yields that all of the bubble's energy has been radiated before the bubble collapses completely. While the approximations under which the integrated far-field acoustic radiation [21] was derived no longer apply as the speed of collapse approaches the speed of sound in water, it is clear that a very large percentage of E_B is radiated as high-frequency sound. This is further suggested by comparing the energy in the bubble at the top of the first afterbounce E_1 to E_B. Typically

one finds $E_1/E_B \sim 2/100$. Thus 98 % of E_B is lost between the maximum radius and the top of the first afterbounce. Obviously the lion's share of this loss is accounted for by acoustic radiation during the collapse to the minimum radius. Simplified theories of SL (Hilgenfeldt, Grossman, & Lohse 1999) based upon applying Rayleigh's equation to the entire collapse violate its domain of applicability and can run into difficulties in accounting for energy balance, in particular the energy remaining in the bubble at the moment of collapse.

The gigahertz sound is absorbed within a few microns of the bubble, and so the dissipated energy density near the bubble is 10^{10} erg/cc, which is huge when compared with the heat density of 10^{-5} erg/cc generated by Kirchoff's law.

The sound under ~10 MHz can propagate out to the boundary and return to the region of the bubble on the next cycle (Holzfuss et al 1998).

The bubble energy lost to viscosity is found from Rayleigh's equation and Equation 9 and scales as

$$E_\eta \sim \sqrt{\frac{3}{2}}\,\frac{16\eta}{\rho R_m}\,\sqrt{\frac{\rho}{P_0}}\,E_B, \tag{22}$$

which is about 4% E_B. This energy winds up in the thermal degrees of freedom of the water.

The energy of the light radiated is $10^{-5}\,E_B$. Overall energy balance is graphed in Figure 10.

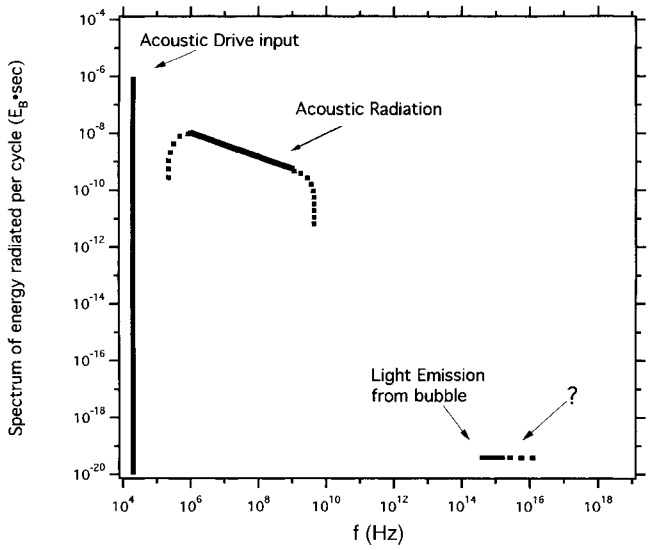

Figure 10 Schematic of energy spectrum radiated by a sonoluminescing bubble.

IMPLODING SHOCK WAVE/PLASMA BREMSSTRAHLUNG MODEL

The strongly supersonic collapse measured in Figures 6 and 7 suggests that an imploding shock wave is launched into the interior of the bubble (Löfstedt et al 1993; Barber & Putterman 1992; Wu & Roberts 1993, 1996; Greenspan & Nadim 1993; Moss et al 1999; Moss et al 1997).

From Rayleigh's equation, one already verifies that the bubble is collapsing supersonically as it passes through R_0:

$$\frac{\dot{R}(R_0)}{c_g} \approx \left[\frac{2}{3\gamma}\frac{\rho_0}{\rho}\left(\frac{R_m}{R_0}\right)^3\right]^{1/2} \approx \mathrm{O}\ (1), \tag{23}$$

where ρ_0 is the ambient gas density. Thus expansion ratios R_m/R_0 of $\sim$10 overcome the small ratio of gas to fluid density and, in general, this is the rough criterion for SL (Barber et al 1994).

This shock front further focuses the energy. In an ideal gas, Guderley (1942) demonstrated that, in the limit of large nonlinearity, there exists a self-similar solution to the Euler equations, where the radius of the imploding shock front

$$R_s(t) = A_i|t|^\alpha, \tag{24}$$

and where for a noble gas $\alpha = 0.7$. Time here is measured from the moment of focusing $R_s = 0$. After imploding, the shock front explodes out through the already shocked gas so that, for $t > 0$,

$$R_s = A_0 t^\alpha, \tag{25}$$

and for the ideal gas, $A_0/A_i = 0.49$. The shock front speeds up as it focuses to the origin and thus further concentrates the energy and increases the temperature. In the Euler approximation, the speed reaches infinity, and the maximum temperature increase that it induces also becomes infinite.

For a van der Waals equation of state, the self-similar solution still works (Wu & Roberts 1994), but A and α depend on the ratio of the van der Waals hard-core density to the density of the gas when the shock forms. For a bubble with $R_0 = 4.5$ μm, driven by a sound field with amplitude 1.275 atm at 26.5 kHz, $\alpha = 0.51$, $A_0/A_i = 4.8$, and $A_i = 5.4$ cm/s$^\alpha$ (Wu & Roberts 1994). In this example the shock front is imploding at Mach 15 (relative to c_0) when it has reached a radius of 0.2 μm at a time 20 ps before focusing. Extrapolating back to the collapsed bubble radius of 0.5 μm, the van der Waals solution implies a velocity of $\sim$Mach 6, consistent with the measured R for the bubble's wall (Barber et al 1997a, Weninger et al 1997, Barber et al 1997b) (Figure 6). The actual shock is nucleated inside the bubble at about half its radius.

For the ideal gas, the heating T/T_0 is roughly proportional to M^2 during the implosion. But upon exploding, the gas is heated again and the temperature rise at that moment approaches M^4 (focusing is a strong shock but expansion is still

self-similar but not a strong shock). In a physical system the key question when this model is applied is, how close to $R_s = 0$ does the shock get before disintegrating? The closer to $R_s = 0$, the greater the heating, and, if the shock should make it down to 50 Å, then local heating is high enough for fusion (Barber et al 1994). Many issues come into play relating to transport processes and equations of state (Vuong & Szeri 1996; Vuong, Szeri, & Young 1999; Stoney & Szeri 1999). A resolution of this issue will depend on experiments or a full-blown molecular-dynamics simulation of the hot spot. In the framework of the shock wave model, the hot region has $\lesssim 10^8$ particles, and so the actual system may be amenable to simulation. Because the gas is very dense, the mean free paths are measured in angstroms, so it may actually be consistent with continuum models to consider shocks as small as 100 Å.

One can now attempt a simple theoretical model of SL (Barber et al 1997; Wu & Roberts 1993, 1994; Putterman 1998; Crum 1994; Hiller et al 1998). The trapped bubble collapses according to Rayleigh's equation. As the velocity of collapse becomes supersonic, there is a handover to an imploding shock wave, which further concentrates the energy. As the shock reaches its minimum radius, there is a sudden and dramatic heating that ionizes the contents of the bubble. The ionization quenches as the shock expands, and the system cools back down through the ionization temperature. Light comes out only while the plasma exists, which accounts for the flash width being independent of color. The means of light emission is thermal Bremsstrahlung from the accelerating free electrons. These electrons will accelerate and radiate light as they collide with the ions. The Bremsstrahlung so generated has a spectral density per unit wavelength λ per unit volume per second as given by (Glasstone & Lovberg 1960)

$$\frac{dP}{d\lambda} = \frac{16\pi^2 e^6 n_e n_i}{\sqrt{3k_B T m_e^{3/2} \boldsymbol{c}^2 \lambda^2}}\, e^{-hc/\lambda k_B T}, \tag{26}$$

where e and m_e are the electron charge and mass, n_e and n_i are the density of free electrons and ions, and $\boldsymbol{c}$ is the speed of light. The degree of ionization x is generally modeled with Saha's equation (Reif 1965):

$$\frac{x^2}{1 - x} = \frac{1}{n\lambda_\chi^3}\, e^{-\chi/k_B T}, \tag{27}$$

where n is the density of particles at temperature T, X is the ionization potential, and the thermal deBroglie wavelength of the electrons is

$$\lambda_\chi = \frac{h}{(2\pi m_e k_B T)^{1/2}}. \tag{28}$$

The spectrum is broad banded and falls off with wavelength in much the same way as the measured spectra. If the shock makes it down to ~0. 1 μm, then the heating (to ~10 eV) is sufficient to explain the observed spectra. At this tem-

perature the contents of the bubble are ionized, and the plasma would have a charge density of $\sim 10^{23}$/cc and a net free charge of $\sim 10^{8}$.

Neither an imploding shock nor a plasma has been observed. Although outgoing pulses have been measured (Barber et al 1997a, Weninger et al 1997, Barber et al 1997b, Matula et al 1998, Wang et al 1999), they would be emitted whether or not there is an imploding shock. So one may ask, is an imploding shock a mandatory aspect of SL (Hilgenfeldt et al 1999, Weninger et al 1997)? The temperature generated by a uniform adiabatic compression (Equations 1, 3) can be high, as shown in Figure 7 (Löfstedt et al 1993, Hilgenfeldt et al 1999). But, in general, this is not high enough to explain the spectrum. Strictly speaking the observation of a spectral peak beyond 6 eV could be consistent with a black-body spectrum with a temperature of ~ 2 eV. But it is hard to explain how photon-matter equilibrium could be set up at such a low temperature within a distance given by the wavelength of light (Kondic et al 1995). For plasma Bremsstrahlung, the light from electrons accelerating owing to collisions with ions simply leaves the inner region of the bubble, and the spectrum observed is the Fourier transform of the individual scattering event!

Considerations of energy balance could also indicate the necessity of an energy-focusing mechanism in addition to the Rayleigh collapse. Take for instance the 6-μm ambient bubble, which contains 2.25×10^{10} molecules and has $E_B \approx 0.5$ erg. For the average temperature to be 2 eV (Hilgenfeldt et al 1999), the bubble must retain 20% of its maximum energy E_B right down to its moment of collapse. But if 0.9 E_B is radiated as sound, which as argued above appears plausible, then on average each molecule has $<3/4$ eV of energy in the collapsed bubble, which is a temperature of $<1/2$ eV, so the efficiency of uniform heating is limited. For a uniform adiabatically compressed bubble, a temperature of 1/2 eV is substantially lower than the few electron volts per atom needed to explain a strongly UV spectrum, but in the shock model, where the average energy in the shock zone is 10 eV, the average over the entire bubble is $<1/10$ eV. Improvements in this attempt to back out an upper bound for the average energy per molecule in the collapsed bubble will require the inclusion of nonlinear corrections to the radiation of sound and the equation of state of water (Prosperetti & Hao 1999). It may be possible to demonstrate theoretically that shocks or some other energy-focusing mechanism is required to explain the observed spectra.

The need for an energy-focusing mechanism in addition to that provided by adiabatic heating of the bubble's interior is also indicated by the remarkable observation that SL from single helium and xenon bubbles in water has very similar properties as illustrated in Figure 9. Although the degree of ionization that is achieved by adiabatic compression (which reaches temperatures of about 1.5eV) differs by a factor of 10^4, SL from helium bubbles is down only by about a factor of 5 from xenon bubbles with the same radius. Theories (Hilgenfeldt et al 1999) which propose that light emission originates in a uniformly heated bubble therefore disagree with experiment by a factor of 10^3. An explanation of the similarity

of helium and xenon bubbles constitutes a key challenge of proposed theories of SL.

Other proposed light-emitting mechanisms include radiation from accelerated zero-point motion (Schwinger 1993, Eberlein 1996, Brevik et al 1999, Milton & Ng 1998) and radiation from quantum tunneling (Willison 1998). The method of light emission could be illuminated if various experimental challenges were overcome. These include a measurement of (*a*) the spectrum beyond 6 eV, (*b*) the electron temperature, (*c*) the ion temperature, which can be hotter than the electron temperature, (*d*) the charge density of the plasma (if it is really a plasma), and (*e*) the size of the light-emitting region.

Indirect evidence for the size of the light-emitting region comes from measurements of the angular dependence of the correlations in the emitted light. If one assumes that these dipolar effects are caused by the refraction of outgoing rays from the hot spot (smaller than the bubble) by the distorted surface of the bubble, then one obtains an estimate of the bubble's size (Weninger et al 1996, Madrazzo et al 1998).

MAXIMIZING SONOLUMINESCENCE

Figure 11 is a waterfall plot of bubble radius as a function of time for increasing drive levels. Note that, as the acoustic drive level increases, the intensity of SL indicated by the ramp also increases, until at some maximum drive level the bubble can no longer be maintained.

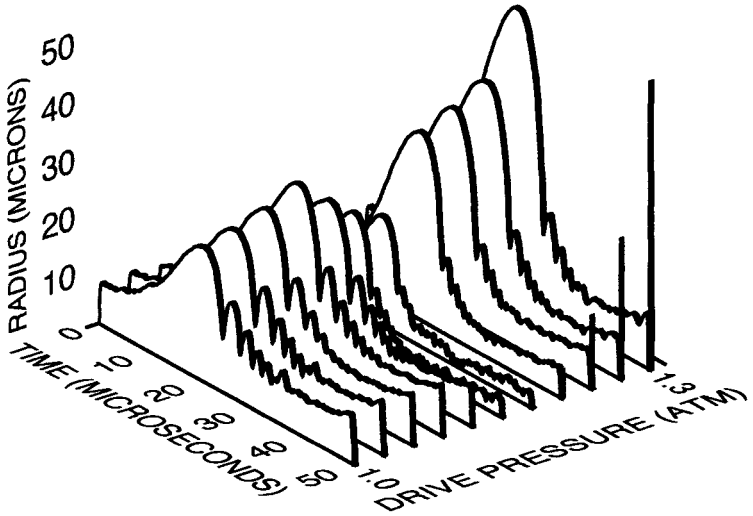

Figure 11 Radius versus time for one cycle of the sound field for increasing drive level for a 5% argon-in-nitrogen mixture dissolved into water at 150 torr. The *vertical bars* display the relative SL intensity.

What is the physical process limiting SL? One possibility is the appearance of large distortions (Brenner et al 1995, Hilgenfeldt et al 1998, Wu & Roberts 1998) such as are a serious concern for inertial confinement fusion. Certainly shape changes play a role in SL. Examples are bubble pinch-off in pure argon bubbles at 150 torr (Barber et al 1995), photos of bubble distortions (Holt & Gaitan 1996, Gaitan 1999), nonisotropic light emission (Weninger et al 1996), and fluctuations in Mie scattering (Weninger et al 1997). Are the shape changes merely another aspect of SL, or are they limiting its effectiveness?

We consider spherical harmonic distortions of the otherwise spherical bubble with average radius as determined by Equation 1:

$$R(t) = \bar{R}(t) + \sum_{n=2}^{\infty} a_l(t) Y_l(\theta, \phi). \tag{29}$$

The time development of a has an ordinary part coupled to a history dependence controlled by diffusion and indicated by D (Wu & Roberts 1998, Prosperetti 1977):

$$R\ddot{a}_l + [3\dot{R} + 2\alpha]\dot{a}_l - \left[(l-1)\ddot{R} - \frac{2\nu(l-1)(l+2)}{R^2}\dot{R} - \omega_\sigma^2\right]a_l = D(R, t) \tag{30}$$

$$\omega_\sigma^2 = \frac{(l-1)(l+1)(l+2)\sigma}{\rho R^3}$$

$$\alpha = \frac{(l+2)(2l+1)\nu}{R^2}. \tag{31}$$

The reversible part of the motion can be transformed with a new variable $y = aR^{3/2}$ to

$$\ddot{y} = y\left(\frac{5\ddot{R}}{2R} + \frac{3\dot{R}^2}{4R^2}\right) = 0. \tag{32}$$

During the collapse, Equation 32 becomes

$$\ddot{y} + y\left(\frac{3A^2}{R^5}\right) = 0, \tag{33}$$

where the constant A is determined by Equation 9. Owing to the fast time scale of the collapse, the positive coefficient of y indicates that this part of the motion is stable, although there can be a geometric scale change in a (Löfstedt et al 1995, Prosperetti 1977). The implosion is not a source of exponential instability, and single shots are linearly stable. Of course this analysis is being carried out in the framework of the low-Mach-number theories and so has the same built-in limitations as the Rayleigh equation.

Can a small net change in a during one cycle then build up over many cycles to destabilize the bubble through the development of a large convoluted surface? This brings in viscosity and requires a more careful discussion of Equation 30. The left-hand side of Equation 30 describes the instantaneous change in a caused by a mechanical viscous effect but neglects the feedback from the diffusion field outside the bubble. The effects of coupling to vorticity diffusion in the water are included in D, which depends on past history. Neglecting diffusion, any increase in a decays exponentially with time as $\exp(-\alpha t)$ (to leading order in viscosity) and will not survive to the next cycle, or even a given cycle. However, the initial value problem for small shape oscillations does not exhibit exponential decay! Over the first few periods the motion does follow $\exp(-\alpha t)$, but soon a diffusion bottleneck is reached, as is shown in Figure 12. After this time the decay is polynomial ($1/t^{5/2}$ for quadrupolar motion), and the shape changes are long lived (Roberts & Wu 1998). For higher viscosity the asymptotes are identical.

Figure 13 shows that the shape changes build up during the afterbounces of the SL collapse. This can be interpreted in terms of the mechanical aspect of the temporal development of a. Two regimes are apparent. When afterbounces are a

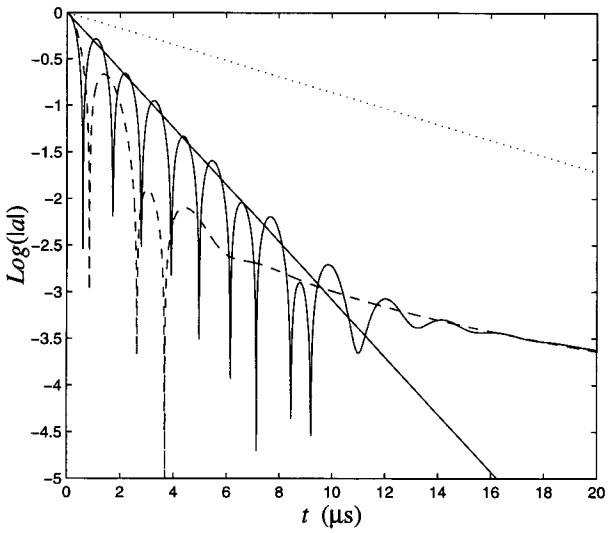

Figure 12 Decay of quadrupolar oscillations of a bubble of radius 4.5 μm, surface tension 73 dynes/cm, and kinematic viscosity 0.01 cm^2/s (*solid curve*), 0.03 cm^2/s (*dashed curve*). The *solid straight line* represents the exponential decay of surface modes (Löfstedt et al 1993), based on calculations that yield exponential decay (Landau & Lifshitz 1987). This result, although valid at short time, deviates from the actual linear response at long times owing to the diffusion bottleneck (or long time tail). The *dashed straight line* calculated from an asymptotic expansion (Brenner et al 1995) that is wrong (Putterman & Roberts 1998) at both short and long times has been used as the basis for predicting (Hilgenfeldt & Lohse 1999) that, at low frequencies, SL would scale up by a factor of 100–1000.

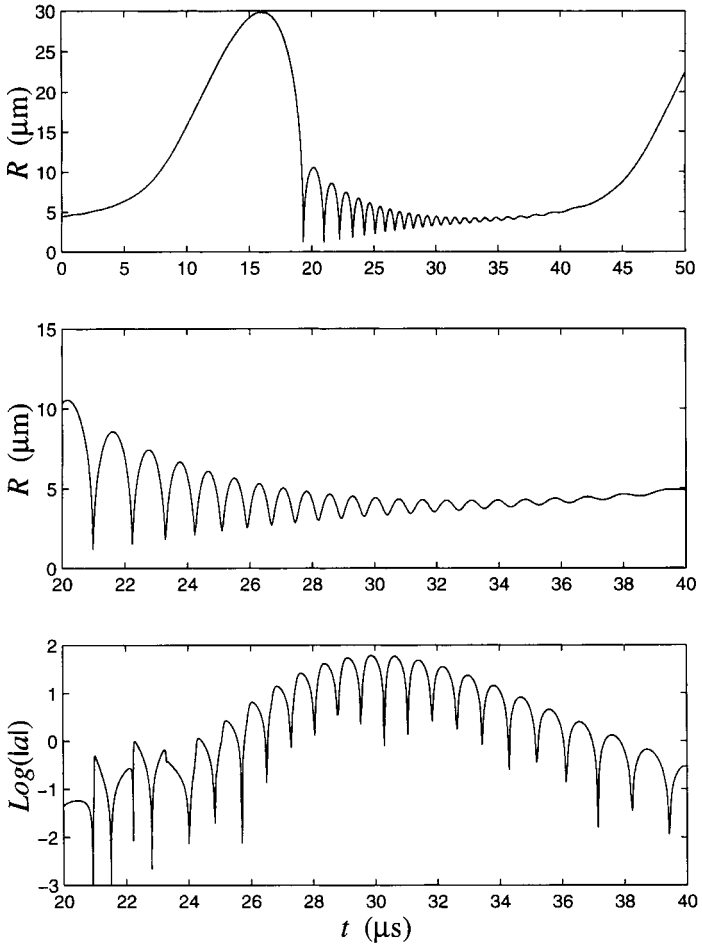

Figure 13 Radius and quadrupolar distortion versus time for a solution to Rayleigh's equation with $R_0 = 4.5$ μm, $P_a = 1.275$ atm, and a heat capacity ratio of 1.4, showing the growth of shape instabilities during the afterbounces.

periodic drive equation, Equation 33 resembles a Matthieu-type equation during that portion of the cycle. Provided that the afterbounce has a sufficient amplitude compared with viscosity, there can be a multiplicative growth. Typically the maximum value of R divided by its minimum value must exceed 2 for a to grow during the afterbounces. Also during the first few ''cuspy'' afterbounces, da/dt can change dramatically at the minimum based on $\Delta\dot{a}/a = \Delta\dot{R}/R$ (CC Wu & PH Roberts, personal communication, 1999). In principle these shape changes can build up from cycle to cycle. But extension of the theory to this case is questionable because it entails integrating through the SL radius, where we do not know

the physics, and surely Rayleigh's equation and linear approximations are invalid. Perhaps one should regard the collapse as inducing some uncontrolled (and, as of now, unpredictable) shape change, which is larger for brighter bubbles; this distortion builds up during the afterbounces so as to destroy the bubble during a given cycle. So the death of the bubble could indeed be caused by a shape distortion, but to pin down its precise location in parameter space once again requires knowledge of the physics of the collapsed state.

Another problem with this picture is presented by bubbles formed in a mixture of glycerine and water. Even for glycerine concentrations that increase the viscosity by a factor of >2 such as when water cooled is to 0°C, the emission of light is unchanged (G Vazquez, unpublished data). If shape instabilities are the key to the maximum level at which SL can be driven, then viscosity is the key parameter; a higher viscosity would imply a greater threshold for afterbounce amplification (see Equation 30). Thus the increase in SL in water as temperature is lowered would be understood in terms of the viscosity increasing, but then glycerine mixtures pose a problem. Of course it is difficult to change only one quantity, and perhaps the glycerine has other consequences, although it must be emphasized that the light emission from the glycerine system is stable. Another problem is that the bubble motion in the real system does not have as many large afterbounces as the Rayleigh equation that is used to simulate the shape distortions. In the real system, afterbounces are damped more strongly owing to thermal diffusion and the effects of impurities in the water. If, in the calculations, the afterbounces are damped out to match the experiment, then the results change significantly. Also, in flow through a Venturi tube, one studies luminescence from a single bubble collapse, and, as with steady-state SL, the intensity increases dramatically as the temperature is lowered (Weninger et al 1999b) (Figure 14). The afterbounces would seem to be irrelevant in this case.

WHAT ARE THE CONTENTS OF THE SONOLUMINESCENCE BUBBLE?

The shock wave theory of SL does not predict the range of drive pressures at which SL exists or the size or contents of the bubble. The model must be supplemented with other processes. As mentioned above, the shape instabilities may provide some insight into the maximum drive level. Here we discuss matters related to the properties of the steady-state bubble.

The law of mass diffusion leads to a steady-state value for the ambient radius that is determined by the strength of the acoustic drive and the concentration c_∞ with which the gas in question is dissolved into the water. When the bubble is expanded, its internal pressure is low compared with the partial pressure in solution

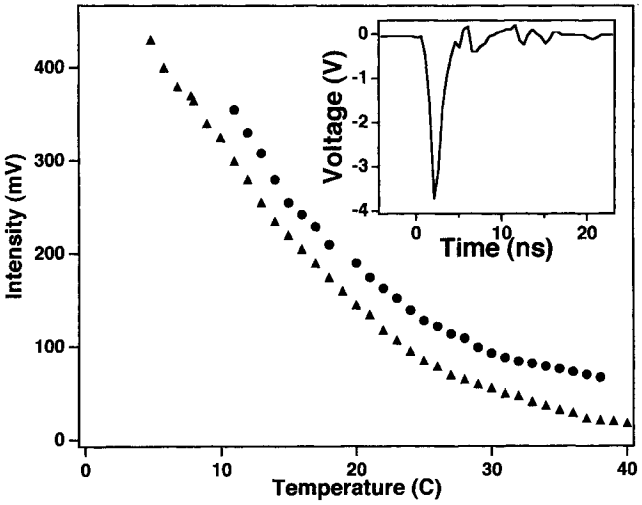

Figure 14 Intensity of light emission as a function of temperature for cavitation induced by flow through a Venturi tube. The inset shows the response of a photomultiplier tube to a single flash, indicating that these events take place on a subnanosecond time scale. Shown are data for water and water with butanol; air has been replaced with xenon gas.

$$p_\infty = p_0 c_\infty / c_0, \tag{34}$$

where c_0 is the saturated concentration at 1 atm, and gas flows into the bubble. When the bubble sits at its ambient radius, the pressure is 1 atm, and gas flows out into the surrounding fluid. The balance between these processes in steady state yields

$$c_\infty / c_0 \approx 3(R_0/R_m)^3, \tag{35}$$

and so the observation of SL from bubbles with $R_m/R_0 = 8$, where gas is dissolved at a 40% concentration, immediately indicates that mass diffusion alone cannot describe SL (Barber et al 1997a, Löfstedt et al 1995, Löfstedt et al 1993). Some other process must be ejecting the extra mass ΔM that diffusion forces into the bubble (total mass M) on each cycle, where (Löfstedt et al 1995)

$$\frac{\Delta M}{M} \approx \frac{3}{2}\left[\frac{T_a D}{R_0^2}\right]\frac{c_\infty}{c_0}\,\frac{c_0}{\rho_0}\,\frac{R_m}{R_0} \approx 2 \times 10^{-4}, \tag{36}$$

and where $c_0/\rho_0 \approx 0.02$; $\rho_0 \approx 10^{-3}$ g/cc; and $D \approx 2 \times 10^{-5}$ cm^2/s is the diffusion coefficient.

From another direction we note that sonoluminescence from a single bubble trapped in a resonant sound field in water is very sensitive to the presence of a noble gas. If the 1% argon that is contained in air is removed, then the light emission and bubble motion become unstable and very dim. Indeed, to see SL

from nitrogen or oxygen requires the presence of some noble gas. In Figure 15 is plotted the ambient radius and acoustic-drive levels for steady-state bubble motion for a 3-mm argon bubble and a 5% argon-in-nitrogen bubble dissolved into water at 150 torr. We see that, in the region of SL, the physical parameters of the 5% argon bubble lie between the calculated parameters for a 3-torr and 8-torr pure argon bubble. This suggests that, in the SL regime, the N_2 is pumped out of the bubble, thus concentrating the argon (Barber et al 1997a, Putterman 1998, Hilgenfeldt et al 1999, Lohse & Hilgenfeldt 1997, Lohse et al 1997, Ketterling & Apfel 1998). In this picture the turn-on time for SL (Figure 16) is the argon rectification time.

Further evidence comes from the temperature dependence of 300-torr and 45-torr bubbles (1% argon in N_2) (G Vazquez, unpublished data). For a fixed concentration, R_m/R_0 stays roughly fixed with T, and this ratio (Figure 17) follows Equation 33 if one assumes that c_∞ refers to the argon concentration (Lohse & Hilgenfeldt 1997). An actual measurement of bubble contents has yet to be made. For given R_m/R_0 and P_a, Rayleigh's equation has a unique solution that determines R_0, provided that we assume that the bubble is pure noble gas, which appears to be reasonable for mixtures with N_2 or O_2, but not with H_2, CH_4, or SF_6.

An appealing picture of why the argon becomes concentrated invokes the wisdom from decades of research on sonochemistry and SL from clouds of bub-

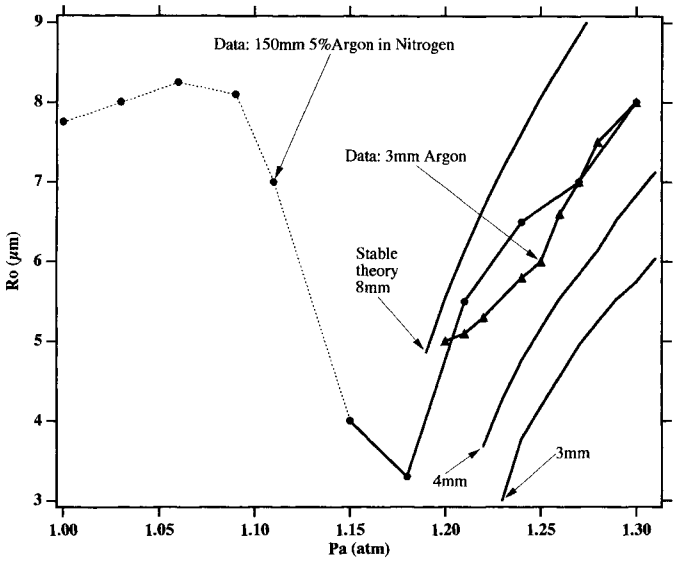

Figure 15 Comparison of measured drive levels and ambient radii for a 3-torr argon bubble and a 150-torr 5% argon-in-nitrogen bubble. In the region of SL, the bubble parameters overlap and furthermore are in reasonable agreement with diffusion theory applied to a pure argon bubble.

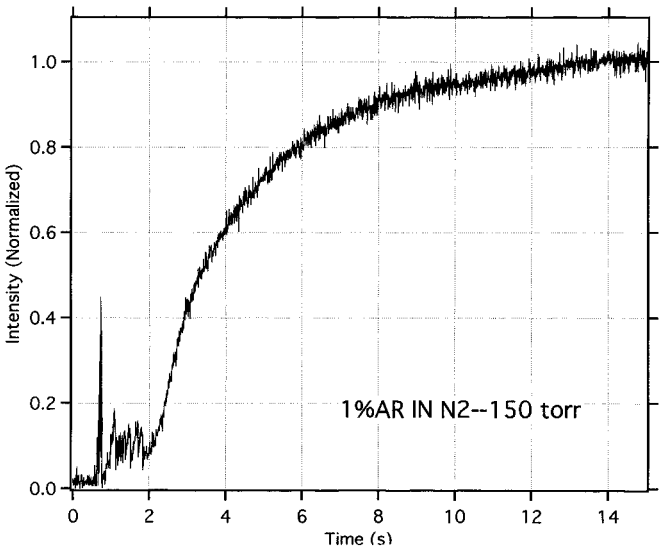

Figure 16 Turn-on time for sonoluminescence showing the light intensity as a function of time after a bubble is seeded into the resonator. The initial (LED) spike indicates the moment when the bubble is seeded. These results confirm the 1970 measurements of Temple.

bles (Walton & Reynolds 1984, Richards & Loomis 1927, Schmitt et al 1929, Beuthe 1932). The energy density generated by the collapse is so great that H_2O, N_2, and/or O_2 become dissociated in the bubble and form new compounds, which are then sucked out into the surrounding water (Hilgenfeldt et al 1999, Lohse & Hilgenfeldt 1997, Lohse et al 1997). For O_2, the new compound would be peroxide, and, for N_2, the new compounds could be NH_3, NO, and so forth. The formation of peroxide in a cavitating system has a long history of study going back to the original experiments (Beuthe 1932). Also the formation of peroxide as occurs with the medical device (Figure 2) has been invoked as a cause for health cautions (Topaz 1998) (the peroxide can cross cell boundaries and form free radicals that presumably damage DNA (Miller et al 1991), at least in vitro if not in vivo. Although there can be no doubt that the energy in the collapsed bubble is sufficient to cause chemical reactions, the key issue is whether the reactions are sufficiently large to affect the bubble motion, albeit on a long time scale.

If the requisite mass ejection (Equation 36) is provided for by chemical reaction, then the reaction products (e.g. peroxide) must be produced in the quantity of $\sim$1 nm/h. If chemical reactions are taking place at this rate, then the energy focused into dissociation of, for example, N_2 or O_2, is $\sim 5 \times 10^7$ eV/cycle, which is about 10-fold the energy going into light (for a 300-torr 10°C bubble; at different regions of parameter space, this factor approaches 100).

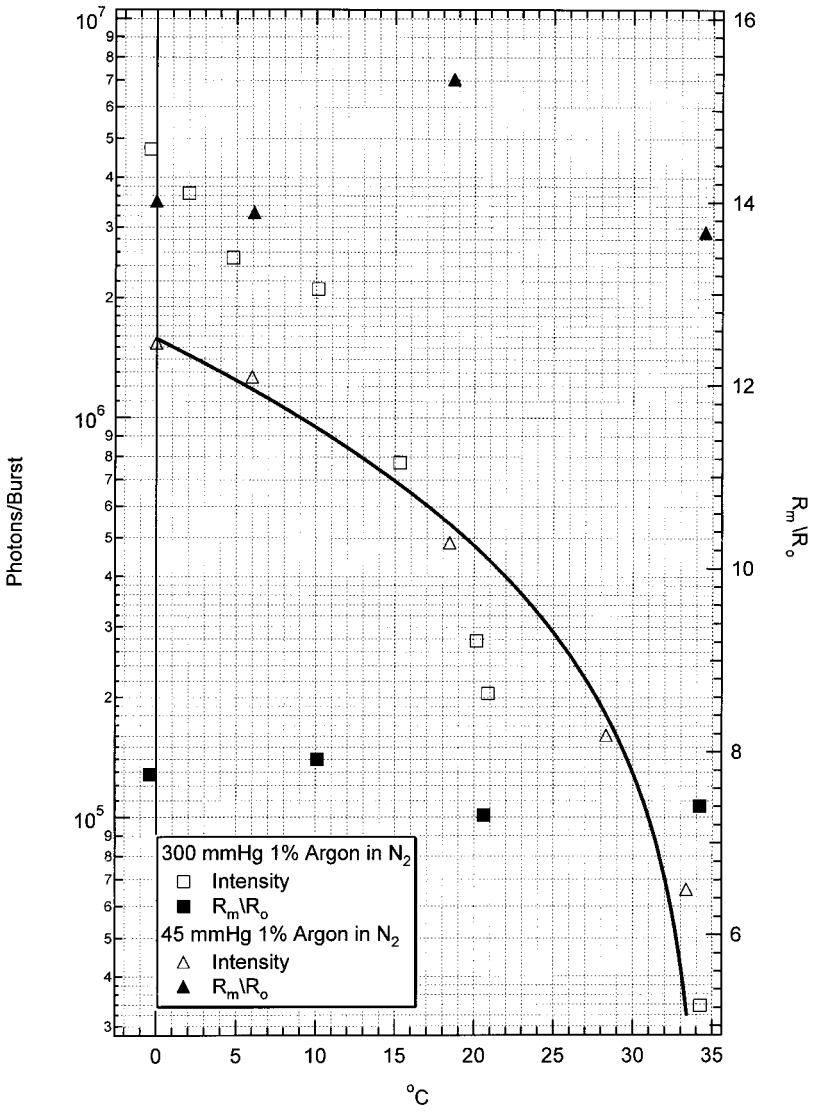

Figure 17 Intensity of sonoluminescence and expansion ratio R_m/R_0 as a function of temperature for 75-torr and 300-torr 1% argon in nitrogen. The major contribution to the increase in SL as temperature is decreased occurs at fixed radius suggesting that vapor pressure is an important parameter (Walton & Reynolds 1984, Moss et al 1999).

To indicate how these issues could be addressed, we consider time scales for dissociation and reaction. In the collapsed bubble, the density is so high that the spacing between atoms or molecules is measured in angstroms. For purposes of

argument, we reckon the mean free path $l \approx 1/(2^{1/2})\, n\sigma_0$ to be $l_c \approx 4$ Å in the collapsed bubble (n is the number density and σ_0 is the collison cross-section). Furthermore, we consider, for the sake of argument, an average temperature of 1 eV and neglect inhomogeneities in the bubble. For an atomic weight of 40, the thermal velocity is 1.7×10^5 cm/s, so that the thermal collision time in the collapsed bubble is $\tau_c \approx 200$ fs.

The dissociation barrier for N_2 is 10 eV, so that, at any given time, only e^{-10} are dissociated. However, if the N_2 is dilute (under the assumption that the argon has been almost rectified), the number N_N of dissociated atoms will accumulate until they collide with each other. That is, in the 1-eV bubble, $\dot{N}_N \sim e^{-10} N_N/\tau_c$ (Lohse & Hilgenfeldt 1997), until the time $\tau_{N-N} \sim (n_{ar}/n_N)^2\tau_c$, which is $10^6\ \tau_c$ (when the diffusive influx of each cycle causes the N_2 to be about a part per thousand) which is larger than the 10^4 collisions required for >10% dissociation. In fact the dissociation is a sizeable fraction of the N_2 in a time of ~2 ns, which (at the level of this calculation) is not unreasonably long compared with the flash of light. If, as mentioned above, the average temperature is only 1/2 eV, then the fraction dissociated by each collisional re-equilibration is reduced to e^{-20}, and the role of dissociation becomes questionable.

The time required for the N_2 to find components of a dissociated water molecule is $\tau_{N-H} \approx (n_{ar}/n_{H_20})^2\tau_c$, which is ~300 ps at 20°C and 4 ns at 0°C, because the vapor pressure drops from 20 torr to 5 torr with this temperature change. If τ_{SL} is the SL flash width that we assume is the lifetime of the hot spot, then for chemical reactions to deplete the inflowing N_2 requires that $\tau_{N-H} > \tau_{SL}$; otherwise, the new compounds would dissociate, and the proper approach would be in terms of chemical equilibrium constants and not activation theory. If this criterion is met at room temperature (which appears possible from our estimates), then it is met by a much larger factor at 0°C. Thus, at 0°C the chemical compounds should be forming for many nanoseconds after the flash is over. The observation of a flux of late photons straggling out at a rate consistent with the quantity of reaction would be a test of the chemical reaction scenario. Another test would entail measurement of the correct quantity of reaction products.

The observation that H_2 bubbles do not display the noble gas doping effect is perhaps consistent with the role of chemical reactions [Hilgenfeldt et al (1999) and Hilgenfeldt & Lohse (1999) appear to claim otherwise], because there are no new final products that can deplete the hydrogen. Nevertheless H_2 bubbles are very dim (by a factor of 20) and less stable than air bubbles (but much more stable than N_2, O_2 pure and bubbles). Experiments that are designed to see a single collapse, such as occurs in cavitation luminescence from flow through a Venturi tube, display very dim emission from diatomics and also the lighter noble gases. So other processes are at work, even if the predictions of the chemical reaction model are verified. Finally, in many nonaqueous fluids, SL is particularly enhanced by xenon gas bubbles (this is also true for the Venturi tube and the medical device in Figure 2, see color insert). The data in Figure 18 show a sample

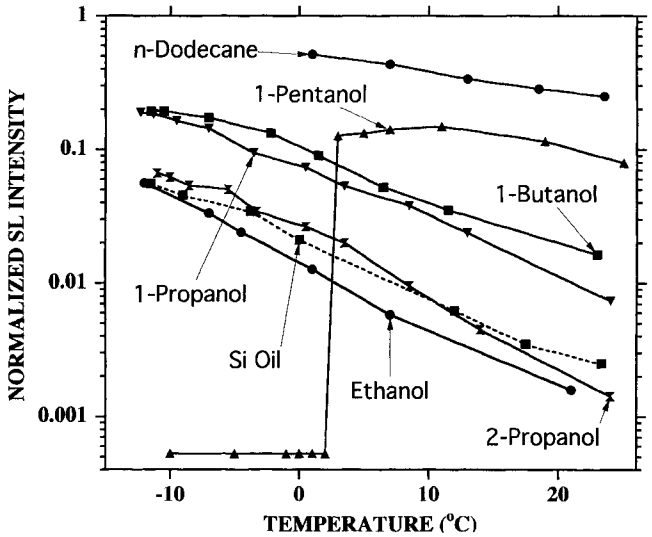

Figure 18 Intensity of sonoluminescence from various nonaqueous fluids as a function of temperature.

of results. In these steady-state systems, one can wonder whether chemical reactions will also lead to a xenon gas doping effect.

Although evidence for argon rectification appears to be strong, the chemical origin of this effect (although appealing) is not yet demonstrated. The possibility of mass segregation (Stoney & Szeri 1999) in the bubble might provide another route to rectification. Finally, SL appears to be very sensitive to impurities (Weninger et al 1995), and the role of the cleanliness of the water has yet to be quantitatively measured (Barber et al 1997a, Maxworthy et al 1996).

CONCLUSION

Suppose a scientist had predicted that the Rayleigh collapse of a bubble would launch an imploding shock wave into its interior such that the bubble contents would compress to the van der Waals hard core and ionize according to Saha's equation and then emit picosecond bursts of UV thermal Bremsstrahlung from a region of a size comparable to the wavelength of light. Suppose that, in addition, he postulated that this phenomenal sequence of events would all be mitigated by the theories of linear-bubble-shape stability, linearized mass diffusion, bubble pinch-off, and chemical reactions. Probably his sanity would be questioned. Not only would it stretch credulity to imagine that the windows of applicability of all these phenomena overlap, but the following would be pointed out:

1. Rayleigh's equation has been applied beyond its domain of derivation. A theory of low-Mach-number motion has been applied to high Mach numbers relative to the bubble and Mach one relative to the water.
2. Saha's equation applies in the ideal gas limit, which is the opposite limit to conditions in the bubble.
3. Bremsstrahlung formulas have been applied to a dense region smaller than or equal to the wavelength of light.
4. Any quantitative results obtained are extremely sensitive to the choices made for equations of state and transport processes.
5. The most mysterious phenomenon of all, namely, that the bubble recovers from the crash to repeat this process with a jitter that has been tuned to less than 35 ps out of 35 μs, has not been addressed. Before the measurement of SL bubble parameters (Barber & Putterman 1992), it had already been claimed that such strongly collapsing bubbles should shatter and disappear upon emerging from the collapse (Prosperetti & Lezzi 1986, 1987). Why does the sum total of all physical processes conspire to allow clocklike oscillations between levels of description, into and out of the realm of hydrodynamics?

This is not to say that the singularity of SL has not driven interesting theoretical advances on topics such as the amplification of quadrupolar motion caused by bubble afterbounces, polynomial long-time decay of linear surface waves, and extension of Guderley's self-similar high-Mach-number solution to the rich domain of the van der Waals equation of state along with stability analysis (Wu & Roberts 1996a,b).

In judging theoretical advances, it is important (and perhaps difficult) to distinguish between a rationalization or parameterization of the data and a predictive advance. The latter might, for example, tell us how to dramatically alter the spectrum, or increase SL by a factor of 100, or obtain a femtosecond flash or an inverted population.

Attempts to rationalize SL should not take away from the search for experimental answers to the key unknowns: the temperature of the electrons and the ions, the free charge density if indeed the bubble becomes a plasma, the maximum degree of energy focusing that can be achieved with this type of process and its extension to laser-induced bubbles (Ohl et al 1998), the degree of coherence or incoherence of the light, and the size of the SL hot spot.

Starting from small-amplitude, long-wavelength initial conditions, an NS fluid sets up a motion that focuses energy density to a degree at which the ''measurements have outstripped the hydrodynamics'' and the ''territory is (still) unknown'' (Maddox 1993).

ACKNOWLEDGMENTS

This research is supported by the National Science Foundation, Division of Atomic Molecular and Optical Physics, and the US Department of Energy, Division of Engineering Research. We are indebted to CC Wu and PH Roberts for

valuable discussions and assistance with Figures 12 and 13. We thank R Vazquez for stimulating discussions and the insights provided by his data (Figure 17). Valuable discussions with KS Suslick are also acknowledged.

LITERATURE CITED

Apfel R. 1986. Possibility of microcavitation from diagnostic ultrasound. *IEEE Trans. Ultrason. Ferroelectr. Freq. Control* 33:139–42

Barber BP, Hiller RA, Arisaka K, Fetterman H, Putterman S. 1992. Resolving the picosecond characteristics of synchronous sonoluminescence. *J. Acoust. Soc. Am.* 91:3061–63

Barber BP, Hiller RA, Löfstedt R, Putterman SJ, Weninger KR. 1997a. Defining the unknowns of sonoluminescence. *Phys. Rep.* 281:65–143

Barber BP, Putterman SJ. 1991. Observation of synchronous picosecond sonoluminescence. *Nature* 352:318–20

Barber BP, Putterman SJ. 1992. Light scattering measurements of the repetitive supersonic collapse of a sonoluminescing bubble. *Phys. Rev. Lett.* 69:3839–42

Barber BP, Weninger K, Putterman SJ. 1997b. Sonoluminescence. *Phil. Trans. R. Soc. London Ser. A* 355:641–48

Barber BP, Weninger KR, Löfstedt R, Putterman SJ. 1995. Observation of a new phase of sonoluminescence at low partial pressures. *Phys. Rev. Lett.* 74:5276–79

Barber BP, Wu CC, Roberts PH, Löfstedt R, Putterman SJ. 1994. Sensitivity of sonoluminescence to experimental parameters. *Phys. Rev. Lett.* 72:1380–83

Beuthe H. 1932. Über den Einfluss der Ultraschallwellen auf Chemische Prozesse. *Z. Phys. Chem.* 163:161–71

Brenner MP, Lohse D, Dupont TF. 1995. Bubble shape oscillations and the onset of sonoluminescence. *Phys. Rev. Lett.* 75:954–57

Brevik I, Marachevsky VN, Milton KA. 1999. Identity of the van der Waals force and the Casimir effect and the irrelevance of these phenomena to sonoluminescence. *Phys. Rev. Lett.* 82:3948–51

Budakian RO, Hiller RA, Weninger KR, Putterman SJ. 1998. Picosecond discharges and stick-slip friction at a moving meniscus of mercury on glass. *Nature* 391:266–68

Crum LA. 1994. Sonoluminescence. *Phys. Today* 9:22–29

Eberlein C. 1996. Sonoluminescence as quantum vacuum radiation. *Phys. Rev. Lett.* 76:3842–45, and comments in *Phys. Rev. Lett.* 77:4690–91(C); 78:2267–70(C)

Frenzel H, Schultes H. 1934. Luminescenz im ultraschallbeschickten Wasser. *Z. Phys. Chem. B* 27:421–24

Gaitan DF. 1999. Sonoluminescence and bubble stability. *Phys. World* 12:20–21

Gaitan DF, Crum LA, Church CC, Roy RA. 1992. Sonoluminescence and bubble dynamics for a single, stable cavitation bubble. *J. Acoust. Soc. Am.* 91:3166–83

Glasstone S, Lovberg RH. 1960. *Controlled Thermonuclear Reactions.* New York: Van Nostrand

Gompf B, Günther R, Nick G, Pecha R, Eisenmenger W. 1997. Resolving sonoluminescence pulse width with time-correlated single photon counting. *Phys. Rev. Lett.* 79:1405–8

Greenspan HP, Nadim A. 1993. On sonoluminescence of an oscillating gas bubble. *Phys. Fluids A* 5:1065–67

Guderley G. 1942. Starke kugelige und zylindrische Verdichtungsstösse in der Nähe des Kugelmittelpunktes bzw. der Zylinderachse. *Luftfahrtforschung* 19:302–12

Hilgenfeldt S, Grossman S, Lohse D. 1999. A simple explanation of light emission in sonoluminescence. *Nature* 398:402–5

Hilgenfeldt S, Lohse D. 1999. Predictions for upscaling sonoluminescence. *Phys. Rev. Lett.* 82:1036–39

Hilgenfeldt S, Lohse D, Moss WC. 1998. Water temperature dependence of single bubble sonoluminescence. *Phys. Rev. Lett.* 80:1332–35; 3164 (E)

Hiller R, Putterman SJ, Barber BP. 1992. Spectrum of synchronous picosecond sonoluminescence. *Phys. Rev. Lett.* 69:1182–84

Hiller R, Weninger K, Putterman SJ, Barber BP. 1994. Effect of noble gas doping in single-bubble sonoluminescence. *Science* 265:248–50

Hiller RA, Putterman SJ, Weninger KR. 1998. Time-resolved spectra of sonoluminescence. *Phys. Rev. Lett.* 80:1090–93

Holt RG, Gaitan DF. 1996. Observation of stability boundaries in the parameter space of single bubble sonoluminescence. *Phys. Rev. Lett.* 77:3791–94

Holzfuss J, Ruggeberg M, Billo A. 1998. Shock wave emissions of a sonoluminescing bubble. *Phys. Rev. Lett.* 81:5434–37

Ketterling JA, Apfel RE. 1998. Experimental validation of the dissociation hypothesis for single bubble sonoluminescence. *Phys. Rev. Lett.* 81:4991–94

Kondic L, Gersten JI, Yuan Chi. 1995. Theoretical studies of sonoluminescence radiation: radiative transfer and parametric dependence. *Phys. Rev. E* 52:4976–90

Landau LD, Lifshitz EM. 1987. *Fluid Mechanics.* Oxford, UK: Pergamon

Löfstedt R, Barber BP, Putterman SJ. 1993. Toward a hydrodynamic theory of sonoluminescence. *Phys. Fluids A* 5:2911–28

Löfstedt R, Weninger KR, Barber BP, Putterman SJ. 1995. Sonoluminescing bubbles and mass diffusion. *Phys. Rev. E* 51:4400–10

Lohse D, Brenner MP, Dupont TF, Hilgenfeldt S, Johnston B. 1997. Sonoluminescing air bubbles rectify argon. *Phys. Rev. Lett.* 78:1359–62

Lohse D, Hilgenfeldt S. 1997. Inert gas accumulation in sonoluminescing bubbles. *J. Chem. Phys.* 107:6986–97

Long GJ, Mautot D, Paulehurst QA, Vandermae D, et al. 1998. Mossbauer-effect and x-ray absorption spectra-study of sonochemically prepared amorphous iron. *Phys. Rev. B* 57:10716–22

Maddox J. 1993. Sonoluminescence in from the dark. *Nature* 361:397

Madrazo A, Garcia N, Nieto-Vesperinas M. 1998. Determination of the size and shape of a sonoluminescent single bubble: theory on angular correlations of the emitted light. *Phys. Rev. Lett.* 80:4590–93

Matula TJ, Hallaj TM, Cleveland RO, Crum LA, et al. 1998. The acoustic emissions from single bubble sonoluminescence. *J. Acoust. Soc. Am.* 103:1377–82

Maxworthy T, Gnann C, Kürten M, Durst F. 1996. Experiments on the rise of air bubbles in clean viscous liquids. *J. Fluid Mech.* 321:421–41

Miller DL, et al. 1991. Ultrasonic cavitation indirectly induces single strand breaks in DNA of viable cells in vitro by the action of residual hydrogen peroxide. *Ultrasound Med. Biol.* 17:729

Milton KA, Ng YJ. 1998. Observability of the bulk Casimir effect: Can the dynamical Casimir effect be relevant to sonoluminescence? *Phys. Rev. E* 57:5504–10

Moss W, Clarke D, Young D. 1997. Calculated pulse widths and spectra of a single sonoluminescing bubble. *Science* 276: 1398–401

Moss WC, Young DA, Harte JA, Levatin JL, et al. 1999. Computed optical emissions from a sonoluminescing bubble. *Phys. Rev. E* 59:2986–92

O'Connor DV, Phillips D. 1984. *Time-Correlated Single Photon Counting.* New York: Academic

Ohl CD, Lindau O, Lauterborn W. 1998. Luminescence from spherically and aspherically collapsing laser-induced bubbles. *Phys. Rev. Lett.* 80:393–96

Picard J. 1676. Sur la lumière du baromètre. *Mem. Acad. R. Sci.* 2:202–3

Peterson FB, Anderson TP. 1967. *Phys. Fluids* 10:874

Prosperetti A. 1977. Viscous effects on perturbed spherical flows. *Q. Appl. Math.* 34:339–52

Prosperetti A. 1984. Physics of acoustic cavitation. *Rend. Soc. Int. Fis.* 93:145–88

Prosperetti A. 1997. A new mechanism for sonoluminescence. *J. Acoust. Soc. Am.* 101:2003–7

Prosperetti A, Hao Y. 1999. Modeling of spherical gas bubble oscillations and sonoluminescence. *Philos. Trans. R. Soc. London Ser. A* 357:203–23

Prosperetti A, Lezzi A. 1986. Bubble dynamics in a compressible liquid. 1. First-order theory. *J. Fluid Mech.* 168:457–78

Prosperetti A, Lezzi A. 1987. Bubble dynamics in a compressible liquid 2. Second-order theory. *J. Fluid Mech.* 185:289–321

Putterman SJ. 1995. Sonoluminescence: sound into light. *Sci. Am.* 272:32–37

Putterman SJ. 1998. Sonoluminescence: the star in a jar. *Phys. World* 11:38–42

Putterman SJ, Roberts PH. 1998. Comment on Bubble shape oscillations and the onset of sonoluminescence. *Phys. Rev. Lett.* 80:3666–67(C)

Rayleigh. 1917. On the pressure developed in a liquid on the sollapse of a spherical cavity. *Phil. Mag.* 34:94–98

Reif F. 1965. *Fundamentals of Statistical and Thermal Physics.* New York: McGraw-Hill

Richards WT, Loomis AL. 1927. The chemical effects of high frequency sound waves I. A preliminary survey. *J. Am. Chem. Soc.* 49:3086–100

Roberts PH, Wu CC. 1998. The decay of bubble oscillations. *Phys. Fluids,* 10:3227–29

Schwinger J. 1993. Casimir light: the source. *Proc. Natl. Acad. Sci. USA* 90:2105

Schmitt FO, Johnson CH, Olson AR. 1929. Oxidations promoted by ultrasonic radiation. *J. Am. Chem. Soc.* 51:370

Stoney BJ, Szeri AJ. 1999. Mixture segregation within sonoluminescence bubbles. *Phys. Fluids.* In press

Suslick KS, Flint EB. 1987. *Nature* 330:553–55

Temple PR. 1970. *Sonoluminescence from the gas of a single bubble.* MS thesis. Univ. Vermont

Terris BD, Stern JE, Rugar D, Mamin HJ. 1989. Contact electrification using force microscopy. *Phys. Rev. Lett.* 63:2669–72

Topaz M. 1998. Possible long term complications in ultrasound assisted lipoplasty induced by sonoluminescence, sonochemistry and thermal effects. *Aesthet. Surg. J.* 18:19

Vuong VQ, Szeri AJ. 1996. Sonoluminescence and diffusive transport. *Phys. Fluids* 8:2354–64

Vuong VQ, Szeri AJ, Young DA. 1999. Shock formation within sonoluminescence bubbles. *Phys. Fluids* 11:10–17

Walton AJ, Reynolds GT. 1984. Sonoluminescence. *Adv. Phys.* 33:595–660

Wang ZQ, Pecha R, Gompf B, Eisenmenger W. 1999. Single-bubble sonoluminescence: investigations of the emitted pressure wave with a fiber optic probe hydrophone. *Phys. Rev. E* 59:1777–80

Weninger KR, Barber BP, Putterman SJ. 1997. Pulsed Mie scattering measurements of the collapse of a sonoluminescing bubble. *Phys. Rev. Lett.* 78:1799–802

Weninger KR, Camara C, Putterman SJ. 1999a. Physical acoustics of ultrasound assisted liposuction. In press

Weninger KR, Camara CG, Putterman SJ. 1999b. Energy focusing in a converging fluid flow. *Phys. Rev. Lett.* In press

Weninger KR, Cho H, Hiller RA, Putterman SJ, Williams GA. 1997. Sonoluminescence from an isolated bubble on a solid surface. *Phys. Rev. E* 56:6745–49

Weninger K, Hiller R, Barber BP, Putterman SJ. 1995. Sonoluminescence from single bubbles in non-aqueous liquids: new parameter space for sonochemistry. *J. Phys. Chem.* 99:14195–98

Weninger KR, Putterman SJ, Barber BP. 1996. Angular correlations in sonoluminescence: diagnostic for the sphericity of a

collapsing bubble. *Phys. Rev. E* 54:R2205–8

Willison J. 1998. Sonoluminescence: proton-tunneling radiation. *Phys. Rev. Lett.* 81: 5430–33

Wu CC, Roberts PH. 1993. Shock wave propagation in a sonoluminescing gas bubble. *Phys. Rev. Lett.* 70:3424–27

Wu CC, Roberts PH. 1994. A model of sonoluminescence. *Proc. R. Soc. London Ser. A* 445:323–49

Wu CC, Roberts PH. 1996a. Structure and stability of a spherical implosion. *Phys. Lett. A* 213:59–64

Wu CC, Roberts PH. 1996b. Structure and stability of a spherical shock wave in a van der Waals gas. *Q. J. Mech. Appl. Math.* 49:501–43

Wu CC, Roberts PH. 1998. Bubble shape instability and sonoluminescence. *Phys. Lett. A* 250:131–36

Figure 2 A metal sphere (4mm diameter) vibrating in water with a peak displacement of about 100μm creates a region of cavitation that transduces the sound into subnanosecond flashes of UV light. For this photo the light emission is enhanced by dissolving xenon into the water.

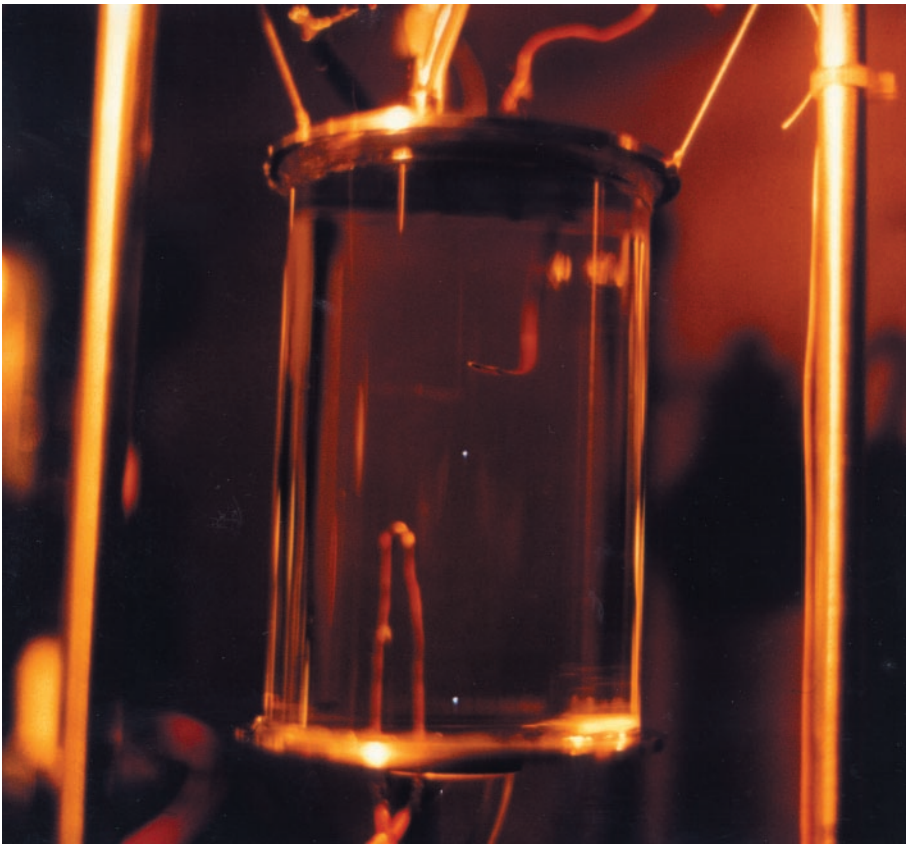

Figure 3 Sonoluminescence from an isolated bubble (or two) trapped by acoustic radiation pressure at the velocity node (pressure antinode) of the sound field. The bubble is seeded with a Nichrome wire which locally boils the fluid, creating vaporous cavities that promptly ingas with whatever gas has been dissolved into the water.

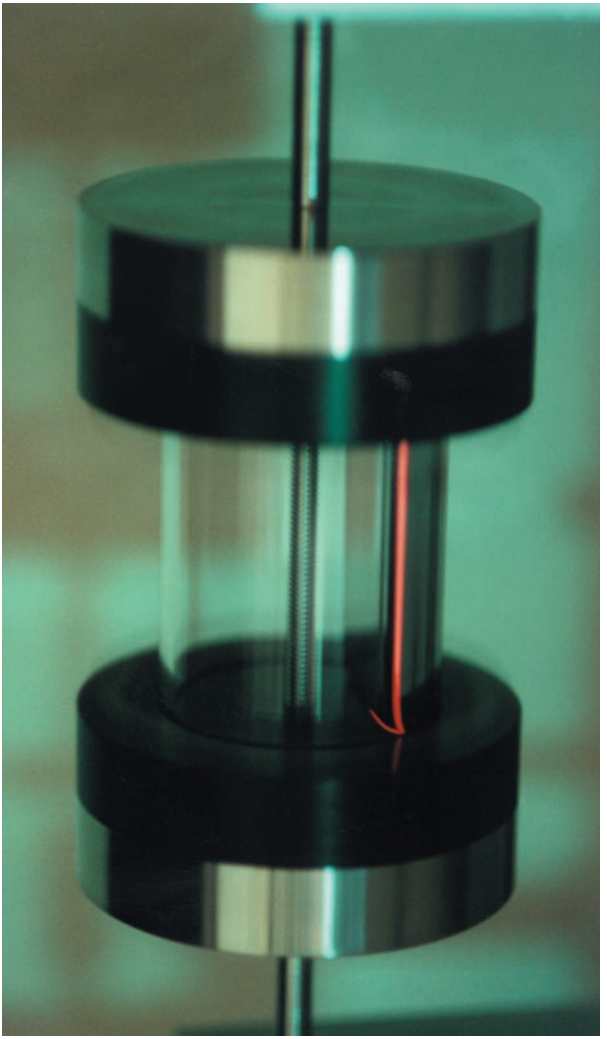

Figure 4 "Barometer Light" (Picard 1676) from the interface of mercury and a rotating wall of glass. The light emission is red due to the presence of neon gas.

Annual Review of Fluid Mechanics
Volume 32, 2000

CONTENTS